

# Polymorphism and solid-gas/solid-solid reactions of isonicotinic acid, isonicotinamide, and nicotinamide copper chloride compounds

*Simon M. Fellows and Timothy J. Prior\**

Chemistry, University of Hull, Cottingham Road, Hull, East Riding of Yorkshire, HU6 7RX, UK.

**ABSTRACT** The crystal structures of 8 new copper chloride coordination complexes with substituted pyridines have been determined through a combination of single crystal X-ray diffraction and *ab initio* structure solution from X-ray powder diffraction data. The polymeric compounds  $[\text{CuCl}_2(\text{INAc})_2]_n$  (**1**),  $[\text{CuCl}_2(\text{INAm})_2]_n$  (**2**), and  $[\text{CuCl}_2(\text{NAM})_2]_n$  (**3**) (INAc = isonicotinic acid; INAm = isonicotinamide; NAM = nicotinamide) consist of chains of  $\text{CuCl}_4$  edge-sharing rhombi decorated by the pyridine-based ligands. All three compounds display similar hydrogen-bonding interactions differing in the arrangement of the polymeric chains. **1**, **2**, and **3** react reversibly with hydrochloric acid in solution/vapour form to produce the corresponding tetrachlorocuprate salts  $[\text{CuCl}_4](\text{H-INAc})_2(\text{H}_2\text{O})$  (**4a**),  $[\text{CuCl}_4](\text{H-INAc})_2$  (**4b**),  $[\text{CuCl}_4](\text{H-INAm})_2$  (form I/form II) (**5a/5b**), and  $[\text{CuCl}_4](\text{H-NAM})_2$  (form I/form II) (**6a/6b**). **4a** exhibits discrete square planar  $[\text{CuCl}_4]^{2-}$  ions, whereas the Cu in **4b**, **5a** and **5b** is in a 4+2 coordination. All four compounds display similar hydrogen bonding arrangements to those found in **1** and **2**. **6a**

and **6b** differ substantially from these compounds in both the hydrogen bonding contacts and the coordination geometry of the cuprate ion (flattened tetrahedral), though they differ from each other only in the orientation of the amide groups and packing arrangements. The formation of **6a/6b** depends on the configuration of nicotinamide in the starting material.

## INTRODUCTION

The sorption of gases by solid-state compounds is a hot topic in chemical research. A large proportion of investigations focus on compounds exhibiting permanent porosity, and specifically the sorption of hydrogen and carbon dioxide.<sup>1-3</sup> However, there has recently been an upsurge in publications on both chemical and physical sorption of gases by non-porous compounds, and the associated structural transformations that take place to allow the uptake and loss of guest molecules.<sup>4-6</sup> Information on these types of reactions is at present extremely limited but is key to understanding the fundamental processes involved, which is especially important from an applications standpoint.

Tetrahalometallate ( $[\text{MX}_4]^{2-}$ ) salts are an interesting variety of compounds that can exhibit thermochromism<sup>7</sup> and the ability to act as liquid crystals.<sup>8</sup> Orpen *et al.*<sup>9</sup> were the first to show that release of HCl molecules from such materials is possible through thermal decomposition of Pt and Pd salts to produce the corresponding neutral coordination complexes. They have also showed that the same elimination reactions occur when similar compounds of Co and Zn are heated in an inert atmosphere or ground with a basic salt, *e.g.* KOH, to yield neutral coordination polymers belonging to a family of compounds of general formula *trans*- $[\text{MX}_2(\text{Rpy})_2]$ <sup>10-12</sup> (M = metal, X = Cl, Br; Rpy = pyridine and substituted pyridine *e.g.* methylpyridine) which can be either discrete, or, through bridging halide ions, polymeric in nature depending on the ligand.<sup>13-15</sup> Additionally, they have proved that control over the polymorphic form of the product can be exerted through the

choice of synthetic method,<sup>11</sup> and that the methods they employ can be used to achieve solvent-free synthesis of metal-carbene complexes.<sup>16</sup> The above reactions do not occur spontaneously in ambient conditions however, whereas Brammer *et al.*<sup>17</sup> have demonstrated that the equivalent reactions with Cu, do. Their work focusses on the tetrahalocuprate salts of halopyridines, loss of HX from which results in neutral complexes of general formula *trans*-[CuX<sub>2</sub>(Xpy)<sub>2</sub>]. They have also showed that the reaction is reversible through exposure to damp and anhydrous HCl and HBr gas, and that mechanochemical synthesis of the cuprate salts can be achieved through grinding of the appropriate copper and pyridinium halide salts.<sup>17-21</sup> They have attempted to understand the mechanisms behind these reactions by utilising the difference in X-ray scattering power of chloride and bromide ions as a tracer, however despite these efforts the reactions are still not fully understood.<sup>18</sup>

Isonicotinic acid (INAc), isonicotinamide (INAm), and nicotinamide (NAM) are three common molecules used in crystal engineering owing to the predictable but flexible hydrogen bonding arrangements they produce.<sup>22-24</sup> We found that reaction of INAc with copper chloride produces a complex belonging to the *trans*-[CuX<sub>2</sub>(Rpy)<sub>2</sub>] family and displays highly predictable intermolecular interactions. This prompted us to investigate similar reactions with the related compounds INAm and NAM to study the robustness of the hydrogen bonding interactions, reaction of the *trans*-[CuX<sub>2</sub>(Rpy)<sub>2</sub>] compounds with hydrochloric acid to produce the tetrachlorocuprate salts, and structural comparison of the products to those made with other d-block metals. Here we present the results of that study.

## EXPERIMENTAL METHODS

All reagents and solvents were purchased from Sigma Aldrich, BDH or Fisher Scientific and used as received. INAc.HCl,<sup>25</sup> INAm.HCl,<sup>23</sup> and NAm.HCl<sup>26</sup> were prepared according to the literature procedures. Elemental Analyses were conducted by the Elemental Analysis Service, Department of Chemistry, University of Hull. Infra-Red (IR) spectra were collected on a Thermo Scientific Nicolet iS5 FT-IR spectrometer fitted with a Thermo Scientific iD7 ATR device. SEM images were collected using a Zeiss EVO60 Scanning Electron Microscope (SEM).

**Synthesis of [CuCl<sub>2</sub>(INAc/INAm/NAm)<sub>2</sub>]<sub>n</sub> (1/2/3).** INAc (0.2462g, 2 mmol), INAm (0.2442g, 2 mmol), or NAm (0.2442g, 2 mmol) was dissolved in methanol (25 mL) with stirring and moderate heating, CuCl<sub>2</sub>·2H<sub>2</sub>O (0.1705 g, 1 mmol) was then added to the solution resulting in a light blue-green precipitate of **1**, **2** or **3** respectively which was subsequently filtered and washed with methanol. **1**, **2** and **3** can also be prepared by grinding of CuCl<sub>2</sub>·2H<sub>2</sub>O and two molar equivalents of INAc, INAm or NAm with several drops of water for **1**, or methanol for **2** and **3**. Single crystals of **1** were prepared by evaporation of a dilute hydrochloric acid solution of the compound. Elemental anal. (%) calcd for **1**: C, 37.86; H, 2.65; N, 7.36. Found: C, 38.08; H, 2.40; N, 7.26. calcd for **2**: C, 38.06; H, 3.19; N, 14.79. Found: C, 37.31; H, 3.07; N, 13.96. calcd for **3**: C, 38.06; H, 3.19; N, 14.79. Found: C, 37.71; H, 2.76; N, 14.19.

**Synthesis of [CuCl<sub>4</sub>](H-INAc)<sub>2</sub>(H<sub>2</sub>O)<sub>2</sub> (4a).** Synthesis of **4a** by the literature procedure does not give a pure product.<sup>27</sup> Synthesis of a pure product could be achieved by grinding of CuCl<sub>2</sub>·2H<sub>2</sub>O (0.1705 g, 1 mmol) and INAc (0.2462g, 2 mmol) with several drops of concentrated hydrochloric acid producing a bright green powder. Elemental anal. (%) calcd for **4a**: C, 29.44; H, 3.29; N, 5.72. Found: C, 29.63; H, 3.35; N, 5.54

**Synthesis of [CuCl<sub>4</sub>](H-INAc)<sub>2</sub> (4b).** A small portion of **1** was transferred to a glass vial. A similar vial was filled with concentrated hydrochloric acid. Both were placed inside a larger vessel which

was capped and sealed. A colour change from light blue-green to bright green was observed with no further change in colour after 3 hours. Elemental anal. (%) calcd for **4b**: C, 31.77; H, 2.67; N, 6.18. Found: C, 32.00; H, 2.71; N, 6.11.

**Synthesis of [CuCl<sub>4</sub>](H-INAm)<sub>2</sub> (5a).** INAm (0.2442 g, 2 mmol) and CuCl<sub>2</sub>·2H<sub>2</sub>O (0.1705 g, 1 mmol) were dissolved in concentrated hydrochloric acid (3 mL). The solution was left to evaporate in a crystallising dish resulting in a few green block crystals and some unidentified material. Pure **5a** can be synthesised by prolonged reaction of **2** with hydrochloric acid vapour over 6 days. Elemental anal. (%) calcd for **5a**: C, 31.91; H, 3.12; N, 12.41. Found: C, 31.26; H, 2.64; N, 11.97.

**Synthesis of [CuCl<sub>4</sub>](H-INAm)<sub>2</sub> (5b).** **5b** was synthesised using the same method to produce **4b**, except using **2** as the starting reagent. A colour change from light blue-green to yellow-green was observed over 3 hours, however the material continues to react and a colour change to bright green **5a** occurs over 6 days upon prolonged exposure to the hydrochloric acid vapour. The reaction of **5b** to **5a** still occurs in ambient conditions but is significantly slower. Elemental anal. (%) calcd for **5b**: C, 31.91; H, 3.12; N, 12.41. Found: C, 31.34; H, 2.58; N, 11.94.

**Synthesis of [CuCl<sub>4</sub>](H-NAm)<sub>2</sub> (6a).** **6a** was synthesised using the same method to produce **5a** except using NAm (0.2442 g, 2 mmol). Using this method produces bright yellow crystals of **6a**, but the compound can also be prepared as a bright yellow powder via grinding of NAm.HCl and CuCl<sub>2</sub>·2H<sub>2</sub>O in a 2:1 molar ratio, a 2:1 ratio of NAm and CuCl<sub>2</sub>·2H<sub>2</sub>O with several drops of hydrochloric acid, or **6b** with several drops of hydrochloric acid. Elemental anal. (%) calcd for **6a**: C, 31.91; H, 3.12; N, 12.41. Found: C, 31.85; H, 2.81; N, 12.16.

**Synthesis of [CuCl<sub>4</sub>](H-NAm)<sub>2</sub> (6b).** **6b** was synthesised using the same method to produce **4b**, except using **3** as the starting reagent. A colour change from light blue-green to yellow was

observed with no further change in colour after 3 hours. Elemental anal. (%) calcd for **6b**: C, 31.91; H, 3.12; N, 12.41. Found: C, 31.54; H, 2.63; N, 11.94.

**Single crystal X-ray diffraction.** Single crystal X-ray diffraction data for **1** were collected via a series of  $\omega$ -scans on an Agilent Technologies SuperNova ES2 diffractometer operating monochromated Cu K $\alpha$  radiation ( $\lambda = 1.5418 \text{ \AA}$ ). The needle crystal was mounted on the goniometer in perfluoropolyalkylether oil using a nylon loop. Integration and processing of data were performed in CrysAlisPro.<sup>28</sup> Diffraction data for **5a**, **6a** and **6b** were collected in a similar fashion on a Stoe IPDS2 image plate diffractometer using monochromated Mo K $\alpha$  radiation ( $\lambda = 0.71073 \text{ \AA}$ ). Crystals were mounted in a similar way but using a glass fibre. Data collection and reduction were performed in X-RED.<sup>29</sup> All single crystal diffraction experiments were performed at 150 K.

Crystal structures were solved within the WinGX<sup>30</sup> suite of programs. Initial solutions were found using dual space methods employed within SHELXT.<sup>31</sup> Full-matrix least-squares refinement was completed with SHELXL-2014/7.<sup>32</sup> Hydrogen atoms were initially positioned geometrically then refined using a riding model, except in the case of **1** and **6b** where data were of sufficient quality to justify refinement of X-H distances subject to restraints to keep the bond lengths of similar chemical species similar. In the case of **5a**, the crystal examined was found to be a non-merohedral twin. Integration of data from each twin domain was performed. An initial solution was obtained using data from the main component followed by refinement using data from both twin domains using the hklf5 formalism. The twin fraction was found to be 0.8824(9):0.1176(9). **6a** was identified as a non-centrosymmetric structure of space group *Pca2*<sub>1</sub>. Use of PLATON<sup>33</sup> did not reveal any missed symmetry to suggest a change of space group. Attempts to solve the structure in the equivalent centrosymmetric space group *Pbcm* failed. The non-centric space group *Pca2*<sub>1</sub>

was thus retained. The structure was refined as an inversion twin with a Flack parameter of 0.41(4). The highest electron density difference peak of 2.05 e/Å<sup>3</sup>, 2.313(1) Å from Cu<sub>2</sub>, arises from minor disorder of the Cu<sub>2</sub> CuCl<sub>4</sub> unit. We have explored modelling this as a second component (refined occupancy is about 6%) but this introduces a large number of extra parameters with no improvement in the quality of fit. We have therefore retained the model with a single component for this ion. Further details are contained in Table 1. ORTEP plots of these structures are found in the ESI.

**Table 1.** Crystal structure data for **1**, **5a**, **6a** and **6b**

Compound	<b>1</b>	<b>5a</b>	<b>6a</b>	<b>6b</b>
Empirical formula	C <sub>12</sub> H <sub>10</sub> Cl <sub>2</sub> CuN <sub>2</sub> O <sub>4</sub>	C <sub>12</sub> H <sub>14</sub> Cl <sub>4</sub> CuN <sub>4</sub> O <sub>2</sub>	C <sub>12</sub> H <sub>14</sub> Cl <sub>4</sub> CuN <sub>4</sub> O <sub>2</sub>	C <sub>12</sub> H <sub>14</sub> Cl <sub>4</sub> CuN <sub>4</sub> O <sub>2</sub>
Formula weight	380.66	451.61	451.61	451.61
Temperature (K)	150(1)	150(1)	150(1)	150(1)
λ (Å)	1.54184	0.71073	0.71073	0.71073
Crystal system	Triclinic	Triclinic	Orthorhombic	Monoclinic
Space group, Z	<i>P</i> $\bar{1}$ , 1	<i>P</i> $\bar{1}$ , 1	<i>Pca</i> 2 <sub>1</sub> , 8	<i>P</i> 2 <sub>1</sub> / <i>c</i> , 4
a (Å)	3.7178(3)	7.4752(10)	14.6164(10)	7.6240(9)
b (Å)	7.4212(5)	7.7741(12)	6.9245(3)	13.7623(11)
c (Å)	12.5699(10)	8.0875(12)	33.9593(17)	16.618(2)
α (°)	76.457(7)	77.452(12)	90	90
β (°)	88.766(7)	69.083(11)	90	94.970(10)
γ (°)	85.737(7)	68.367(11)	90	90
V (Å <sup>3</sup> )	336.23(5)	406.10(11)	3437.1(3)	1737.1(3)
Density (Mg m <sup>-3</sup> )	1.880	1.847	1.745	1.727
μ (mm <sup>-1</sup> )	6.126	2.015	1.904	1.884
F(000)	191	227	1816	908
Crystal size (mm)	0.17 x 0.05 x 0.02	0.31 x 0.22 x 0.06	0.49 x 0.25 x 0.12	0.37 x 0.18 x 0.16
θ range (°)	6.15-72.62	2.71-29.49	2.40-29.24	1.92-29.24
Reflections collected	1764	7972	14476	10952
Independent reflections (R int)	1271 (0.0157)	7972 (0.0628)	7931 (0.0454)	4571 (0.0247)
Data/restraints/parameters	1271/6/103	7972/0/107	7931 / 1 / 416	4571/35/220
Goodness-of-fit on F <sup>2</sup>	1.103	0.906	0.885	0.929
R1 [I > 2σ(I)]	0.0280	0.0502	0.0427	0.0233
wR2 (all data)	0.0759	0.1569	0.1051	0.0558

**X-ray powder diffraction.** X-ray powder diffraction (XRPD) data were collected on a PANalytical Empyrean Series 2 diffractometer operating with monochromated Cu K $\alpha_1$  radiation ( $\lambda = 1.54056 \text{ \AA}$ ). Routine experiments were performed in Bragg-Brentano geometry (reflection), however for structure solution and refinement samples were mounted in 0.5 mm borosilicate glass capillaries and data collected in a Debye-Scherrer geometry (transmission).

Diffraction patterns of **2**, **3**, **4b** and **5b** were indexed using the Treor, ITO, Dicvol or Dicvol04 algorithms implemented within HighScorePlus.<sup>34</sup> Candidate cells were further tested by a Pawley fit conducted in the same program. Structure solution was then attempted in each case via the global optimisation via simulated annealing approach in Endeavour.<sup>35</sup> Initial geometries were derived from similar molecules contained within the Cambridge Structural Database (CSD).<sup>36</sup> The initial solutions were then used as the starting point for Rietveld refinement which was conducted using the EXPGUI interface for GSAS.<sup>37</sup> Atomic positions were refined subject to restraints to keep atomic distances similar to those found in similar compounds on the CSD. A single isotropic displacement parameter was refined for all atoms. In the final stage of refinement, hydrogen atoms were placed geometrically and fixed in position for the final calculation cycles with an isotropic displacement parameter set 1.2 times larger than the non-H atoms. A typical profile fit is shown in the text; all other Rietveld fits and powder diffraction data are contained in the ESI. Further details are contained in Table 2.

**Table 2.** Structure refinement data for **2**, **3**, **4b** and **5b**

Compound	<b>2</b>	<b>3</b>	<b>4b</b>	<b>5b</b>
Empirical formula	C <sub>12</sub> H <sub>12</sub> Cl <sub>2</sub> CuN <sub>4</sub> O <sub>2</sub>	C <sub>12</sub> H <sub>12</sub> Cl <sub>2</sub> CuN <sub>4</sub> O <sub>2</sub>	C <sub>12</sub> H <sub>12</sub> Cl <sub>4</sub> CuN <sub>2</sub> O <sub>4</sub>	C <sub>12</sub> H <sub>14</sub> Cl <sub>4</sub> CuN <sub>4</sub> O <sub>2</sub>
Formula weight	378.71	378.71	453.6	451.63
Temperature (K)	293(1)	293(1)	293(1)	293(1)
$\lambda$ (Å)	1.54056	1.54056	1.54056	1.54056
Crystal system	Monoclinic	Monoclinic	Monoclinic	Triclinic
Space group, Z	<i>C2/c</i> , 4	<i>P2<sub>1</sub>/c</i> , 2	<i>P2<sub>1</sub>/c</i> , 2	<i>P</i> $\bar{1}$ , 1
a (Å)	24.319(8)	3.7851(5)	7.6430(5)	3.9177(6)

b (Å)	3.7547(13)	13.868(2)	10.8232(6)	7.7707(11)
c (Å)	16.432(6)	13.115(2)	12.2250(8)	13.778(2)
$\alpha$ (°)	90	90	90	94.070(3)
$\beta$ (°)	111.753(3)	91.680(3)	126.2554(10)	97.408(3)
$\gamma$ (°)	90	90	90	100.338(2)
V (Å <sup>3</sup> )	1393.6(13)	688.1(2)	815.48(12)	407.3(2)
Density (Mg m <sup>-3</sup> )	1.841	1.828	1.847	2.101
$\mu$ (mm <sup>-1</sup> )	1.47	1.47	2.28	2.14
Sample shape (mm)	cylinder 12 x 0.5 x 0.5			
$\theta$ range (°)	2.5-55	2.5-55	2.5-55	2.5-55
Data	3997	3997	4037	4037
Parameters Refined	76	64	64	71
R <sub>p</sub>	0.0654	0.0412	0.0407	0.0347
R <sub>wp</sub>	0.0975	0.0556	0.0573	0.0497

$$R_p = \frac{\sum |I_o - I_c|}{\sum I_o}; R_{wp} = \frac{\sum w(I_o - I_c)^2}{\sum wI_o^2}$$

## RESULTS AND DISCUSSION

### Crystal structures of [CuCl<sub>2</sub>(INAc)<sub>2</sub>] (1), [CuCl<sub>2</sub>(INAm)<sub>2</sub>] (2), and [CuCl<sub>2</sub>(NAm)<sub>2</sub>] (3).

Crystals of [CuCl<sub>2</sub>(INAc)<sub>2</sub>] (1) were initially produced serendipitously from a weak hydrochloric acid solution of copper chloride and INAc, but bulk material can be formed by mixing the same components in methanol. Single crystals of **1** were sent to Agilent Technologies for X-ray diffraction data collection. The compound was found to crystallise in the centrosymmetric triclinic space group  $P\bar{1}$ . The asymmetric unit contains one chloride ion, a neutral INAc molecule, and a copper ion located on the 1a Wyckoff position. As seen in Figure 1A, the structure consists of a chain of edge-sharing CuCl<sub>4</sub> rhombi along the *a* axis with two pairs of different Cu-Cl distances (Cu-Cl 2.8979(6) Å and 2.2842(5) Å). Each copper is further coordinated by INAc above and below the plane. The orientation of the polymer is such that the carboxylic acid groups of two INAc molecules, related by the inversion centre at  $\frac{1}{2}, \frac{1}{2}, \frac{1}{2}$ , create an R<sub>2</sub><sup>2</sup>(8) interaction composed of two O-H...O contacts (O...O 2.629(2) Å) which through the coordinated copper forms part of

a  $C_1^1(14)$  chain running in the  $[\bar{1}11]$  direction. The coordination and hydrogen bonds combine to create a 2-D supramolecular framework shown in Figure 1B. Amazingly the structure **1** is almost identical to that of  $[PdCl_2(INAc)_2]$  despite the absence of a polymeric metal halide chain as Pd is stable in a square planar geometry.<sup>38</sup> Additionally, a pseudohalide analogue of **1** containing Ni,  $[Ni(SCN)_2(INAc)_2]_n$ , is known, although the polymeric chain of the analogue is not as linear as in **1** and is instead puckered which creates voids that can be filled with aromatic guest molecules.<sup>39,40</sup> The aromatic guests appear to make up for the shortcomings in the crystal packing efficiency of  $[Ni(SCN)_2(INAc)_2]_n$ . Since **1** is very densely arranged, it is unlikely to possess similar host-guest properties.

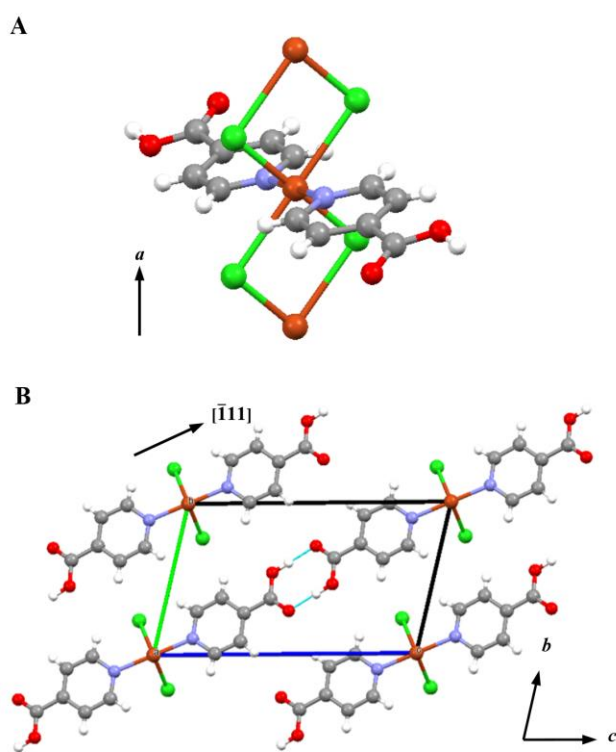


**Figure 1.** The copper chloride chain present in  $[CuCl_2(INAc)_2]$  (**1**) extending along the  $a$  axis (A), and the crystal packing of **1** showing the O-H $\cdots$ O contacts forming a ring type hydrogen

bonding arrangement, and the resulting chain which runs in the  $[\bar{1}11]$  direction (B). Hydrogen bonds are drawn as light-blue dashed lines.

The equivalent compounds formed with isonicotinamide,  $[\text{CuCl}_2(\text{INAm})_2]$  (**2**), and nicotinamide,  $[\text{CuCl}_2(\text{NAM})_2]$  (**3**), could only be produced as powders, but it was possible to index the diffraction patterns as belonging to monoclinic cells of space groups  $C2/c$  and  $P2_1/c$  respectively. Structure solution and refinement from powder data yielded two structures very similar to that observed for **1**. The contents of the asymmetric unit are the same, except for the change of INAc for INAm and NAM. Both compounds exhibit almost identical supramolecular frameworks extending to 3-D through additional N-H $\cdots$ Cl contacts.

The initial structure solution of **2** and subsequent Rietveld refinement against the observed diffraction data gave a good fit ( $R_{\text{wp}} = 0.0975$ ). The Cu atom is sited at the 4a Wyckoff position. Edge-sharing  $\text{CuCl}_4$  rhombi produce a chain extending along  $b$ , as seen in Figure 2A, although the difference in the pairs of Cu-Cl distances is much more pronounced than in **1** (Cu-Cl 2.340(7) Å and 2.843(7) Å). The INAm molecules which decorate the chain produce an  $R_2^2(8)$  interaction composed of two N-H $\cdots$ O contacts (N $\cdots$ O 2.9943(8) Å) between amide groups related by a centre of inversion. As shown in Figure 2B, this forms part of a  $C_1^1(14)$  chain via the coordinated Cu atoms, running in the  $[221]$  direction. Additionally, N-H $\cdots$ Cl interactions (N $\cdots$ Cl 3.3125(9) Å) between amide groups and adjacent Cl ions bridged by Cu combine with the  $R_2^2(8)$  ring motif to produce a  $C_3^2(10)$  interaction along  $a$ . Thus **2** contains sheets in the  $xz$  plane sustained by coordination bonds and hydrogen bonds; perpendicular to these sheets are the  $\text{CuCl}_2$  polymers, hence **2** contains a supramolecular 3-D network. The structure of **2** is very similar to that of  $[\text{CoCl}_2(\text{INAm})_2]_n$  except the Co ion is in a non-distorted octahedral coordination geometry.<sup>41</sup> A

pseudohalide analogue of **2** is also known,  $[\text{Ni}(\text{SCN})_2(\text{INAm})_2]_n$ , which contains voids filled with aromatic guest molecules due to poor packing efficiency as a result of the alternate orientations of the INAm molecules along the  $\text{Ni}(\text{SCN})_2$  chain.<sup>42</sup> Like **1**, **2** is very densely arranged so it is unlikely to accommodate similar molecules.

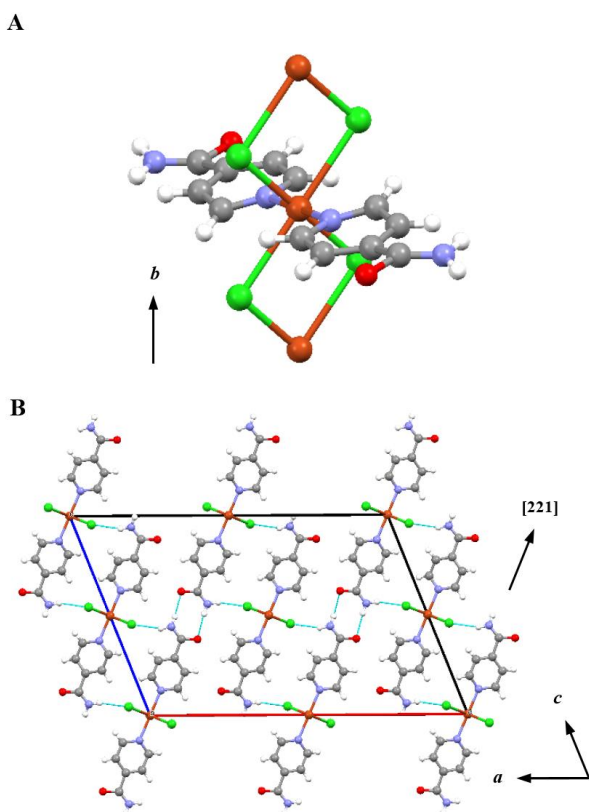


**Figure 2.** The copper chloride chain displayed in  $[\text{CuCl}_2(\text{INAm})_2]$  (**2**) extending along the  $b$  axis (A), and the crystal packing of **2** showing the  $\text{N-H}\cdots\text{Cl}$  and  $\text{N-H}\cdots\text{O}$  contacts, producing the ring type hydrogen bonding arrangement and the two chain interactions that propagate along  $a$  and in the  $[221]$  direction (B). Hydrogen bonds are drawn as light-blue dashed lines.

The unit cell and structure of **3** were determined from powder diffraction data giving an excellent fit to the experimental data ( $R_{\text{wp}} = 0.0556$ ), as shown in Figure 3. The structure of **3** is similar to that of  $[\text{CuCl}_2(3\text{-CNpy})_2]$ <sup>13</sup> and  $[\text{CuCl}_2(3\text{-Xpy})_2]$ <sup>17</sup> but almost identical to  $[\text{PdCl}_2(\text{NAC})_2]$ <sup>38</sup> (NAC

= Nicotinic acid). The Cu atom is positioned on the 2a Wyckoff site and the polymeric copper chloride chain extends along the *a*-axis, as shown in Figure 4A. The short Cu-Cl bond length is comparable to that observed for similar compounds, however the longer bond is rather extended in comparison and might not be considered a formal bond (Cu-Cl 2.298(3) Å and 2.973(3) Å). The polymeric unit in **3** is rotated around *a* when compared to the compounds of 3-CNpy and 3-Xpy, presumably to maximise the strength of intermolecular forces.  $R_2^2(8)$  interactions are present at the centres of inversion at  $(\frac{1}{2}, \frac{1}{2}, 0)$  and  $(\frac{1}{2}, 0, \frac{1}{2})$  between amide groups (N $\cdots$ O 2.932(11) Å), and through the coordinated Cu atoms these create  $C_1^1(12)$  chains along the *b* axis as seen in Figure 4B. Furthermore, an N-H $\cdots$ Cl contact (N $\cdots$ Cl 3.506(8) Å) is observed between amine groups and nearby chloride ions, combination with the ring motif and the bridging of Cl ions by Cu produces  $C_2^2(8)$  interactions along *c*. In a similar way to **2**, compound **3** contains a 3-D supramolecular network composed of sheets that are joined by the CuCl<sub>2</sub> chains.

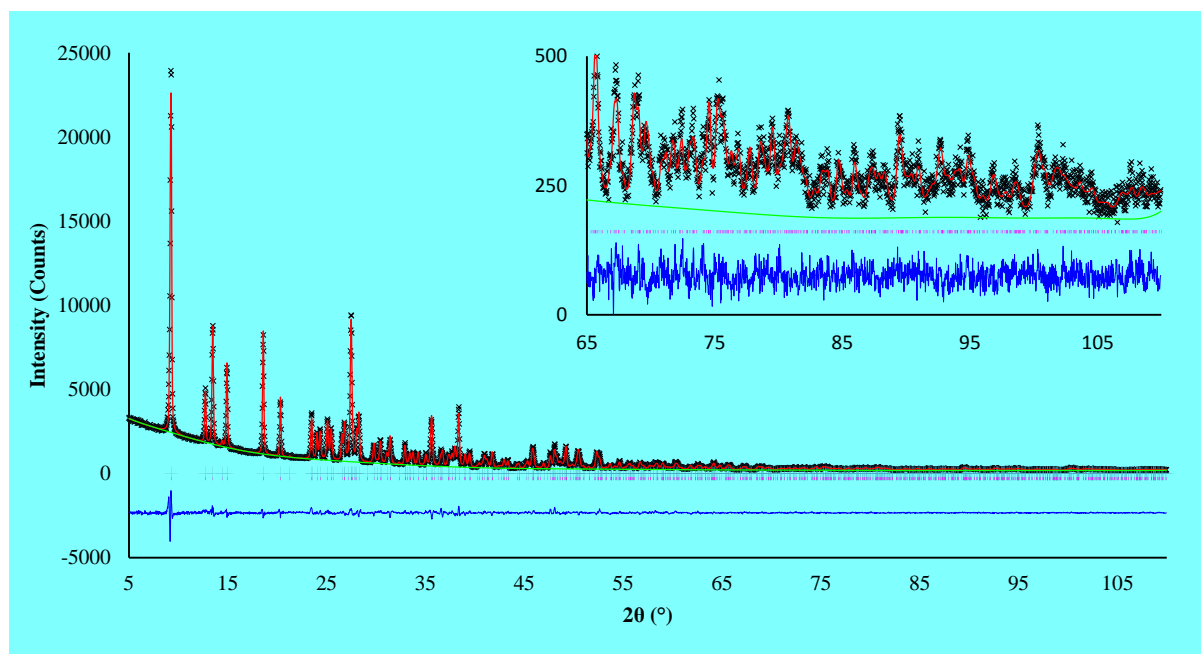


**Figure 3.** A plot of the Rietveld refinement of  $[\text{CuCl}_2(\text{NAm})_2]$  (**3**). Black crosses represent observed data, the red line calculated data, the green line background, the pink markers peak positions, and the blue line is the difference plot  $[(I_{\text{obs}} - I_{\text{calc}})]$ . The inset shows the portion of data between  $65$  and  $110^\circ 2\theta$ .

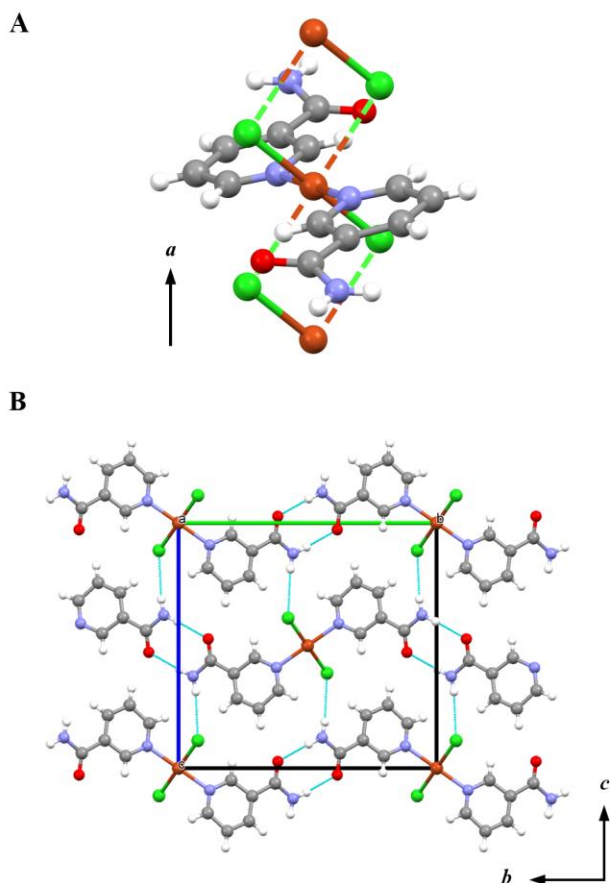


**Figure 4.** The copper chloride chain displayed in  $[\text{CuCl}_2(\text{NAm})_2]$  (**3**) extending along the  $a$  axis (A), and the crystal packing of **3** showing the  $\text{N-H}\cdots\text{Cl}$  and  $\text{N-H}\cdots\text{O}$  contacts resulting in a ring type hydrogen bonding arrangement and two chain interactions running along  $b$  and  $c$  (B). Long  $\text{Cu-Cl}$  contacts are drawn as dashed lines as their length might indicate the absence of a formal bond. Hydrogen bonds are drawn as light-blue dashed lines.

**Cuprate compounds and solid-gas reactions of isonicotinic acid.** Recrystallisation of  $[\text{CuCl}_2\text{INAc}]$ , **1**, from hydrochloric acid produces a green compound,  $[\text{CuCl}_4](\text{H-INAc})_2(\text{H}_2\text{O})$  (**4a**), which has been described previously.<sup>27</sup> It is unexpected that Cu adopts a square planar geometry similar to the Pt and Pd analogues,<sup>25</sup> as opposed to the more common and highly distorted 4+1 and 4+2 geometries. The geometry of Cu is most likely stabilised through strong hydrogen bonds which remove charge from the Cl ions reducing anion-anion repulsion therefore allowing ligand field stabilisation energy to dictate the geometry of the Cu ion; because of this stability, Cu forms no extra bonds thus acting like Pt/Pd. We found that the synthesis of **4a** by the reported method gave an impure compound, however grinding copper chloride and INAc in a 1:2 molar ratio with several drops of concentrated hydrochloric acid gave a compound with no identifiable impurities.

The reaction of **1** with damp hydrochloric acid vapour induces a colour change from blue to bright green in around 3 hours. The compound,  $[\text{CuCl}_4](\text{H-INAc})_2$  (**4b**), has a similar colour to **4a**, though displays a substantially different X-ray powder diffraction pattern. It was possible to index the pattern with a monoclinic cell of space group  $P2_1/c$  with a volume of  $\sim 820 \text{ \AA}^3$ , equivalent to an asymmetric unit of one protonated INAc molecule and half a centrosymmetric planar  $[\text{CuCl}_4]^{2-}$  ion, as in **4a**, with the Cu positioned on a centre of inversion. *Ab initio* structure solution was performed using this simple structural model and an excellent fit to the observed data was obtained by Rietveld refinement ( $R_{\text{wp}} = 0.0573$ ). The identification of **4b** as the anhydrous cuprate is confirmed by elemental analysis. The pyridinium N-H group of INAc forms bifurcated hydrogen bonds to two Cl ions ( $\text{N}\cdots\text{Cl}$  3.1808(2)  $\text{Å}$  and 3.1823(2)  $\text{Å}$ ) of a  $[\text{CuCl}_4]^{2-}$  ion (Cu-Cl 2.2595(1)  $\text{Å}$  and 2.2690(1)  $\text{Å}$ ) producing an  $R_1^2(4)$  motif. Two O-H $\cdots$ O hydrogen bonds (O $\cdots$ O 2.6876(2)  $\text{Å}$ ) between carboxylic acid groups form an  $R_2^2(8)$  interaction. The two ring-shaped arrangements

combine to produce a  $C_3^3(18)$  chain which runs in the  $[102]$  direction, as shown in Figure 5. The chain motifs stack in such a way that long Cu-O bonds ( $3.086(11)$  Å) exist between each copper atom and the carboxylic acids directly above and below it in the  $[501]$  direction, meaning the Cu ion is actually in a 4+2 coordination, also shown in Figure 5. The reason for the formation of the long Cu-O bonds is that the stabilisation of the square planar geometry through hydrogen bonding is reduced, relative to **4a**, by the absence of water. The Cu centre compensates for this loss by formation of long coordinate bonds. The non-hydrated  $[PtCl_4]^{2-}$  salt of INAc possesses very similar hydrogen bond interactions to that observed in **4b**, but because Pt is much more stable in a square planar coordination geometry, no Pt-O bonds are formed and as a result the crystal packing is different.<sup>25</sup> Interestingly, grinding of  $CuCl_2 \cdot 2H_2O$  with two molar equivalents of INAc.HCl produces a green compound with a different diffraction pattern from either the anhydrous or hydrated phases identified thus far. We have been unable to index the powder pattern, and no further characterisation has been conducted. On exposure to air, **4a** and **4b** convert into **1** in around 36-48 hours by release of water and HCl (**4a**), or just HCl (**4b**).

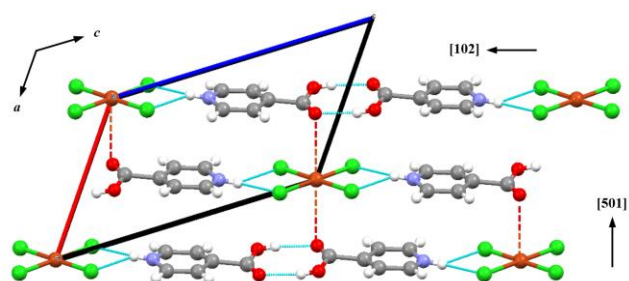


**Figure 5.** The  $C_3^3(18)$  chain interactions in  $[CuCl_4](H-INAc)_2$  (**4b**) that extend in the  $[102]$  direction, and the stacking arrangement of the chains along the  $[501]$  direction to create long Cu-O bonds drawn as dashed lines. Hydrogen bonds are drawn as light-blue dashed lines.

**Cuprate compounds and solid-gas reactions of isonicotinamide.**  $[\text{CuCl}_2(\text{INAm})_2]$ , **2**, can be crystallised from concentrated hydrochloric acid as the cuprate  $[\text{CuCl}_4](\text{H-INAm})_2$  (Form I), **5a**. Green crystals of the compound were analysed by single crystal X-ray diffraction. **5a** adopts a triclinic cell with space group  $P\bar{1}$  and has a very similar structure to **4b**. The asymmetric unit contains a square planar  $[\text{CuCl}_4]^{2-}$  ion with the Cu centred on the 1a Wyckoff position (Cu-Cl 2.2622(4) Å and 2.2960(4) Å) and one protonated isonicotinamide molecule. The pyridinium group of H-INAm forms bifurcated hydrogen bonds to two chloride ions (N $\cdots$ Cl 3.1690(5) Å and 3.1913(5) Å) of a  $[\text{CuCl}_4]^{2-}$  ion producing an  $R_1^2(4)$  motif, while the amide groups form an  $R_2^2(8)$  interaction as seen before (N $\cdots$ O 2.8463(5) Å). The two ring interactions produce a  $C_3^3(18)$  chain which runs in the  $[\bar{1}2\bar{2}]$  direction, shown in Figure 6A. An extra hydrogen bond is observed between amine groups and chloride ions (N $\cdots$ Cl 3.4236(6) Å) which in combination with the  $C_3^3(18)$  interaction forms hydrogen bonded sheets which are parallel to the (212) crystallographic plane. As seen in Figure 6B, the 4+2 coordination observed in **4a** is present here also, long Cu-O bonds (2.986(5) Å) occur between the carboxyl moiety of the amide groups occurring above and below each copper centre along the  $[3\bar{1}1]$  direction.

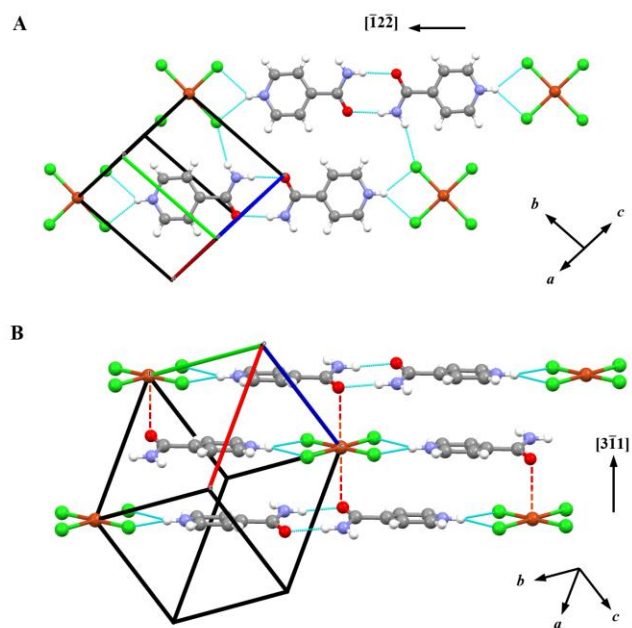


**Figure 6.** A view of the hydrogen bonded sheets in  $[\text{CuCl}_4](\text{H-INAm})_2$  (Form I) (**5a**) as viewed normal to the plane showing the  $\text{C}_3^3(18)$  chain interactions that extend in the  $[\bar{1}\bar{2}\bar{2}]$  direction, and the additional  $\text{N-H}\cdots\text{Cl}$  contacts which link them (A). The stacking arrangement of the sheets in the  $[3\bar{1}\bar{1}]$  direction to create long  $\text{Cu-O}$  bonds drawn as dashed lines (B). Hydrogen bonds are drawn as light-blue dashed lines.

The reaction of **2** with damp hydrochloric acid vapour initially produces a polymorph of **5a**,  $[\text{CuCl}_4](\text{H-INAm})_2$  (Form II) (**5b**), which transforms into **5a** in approximately 6-7 days upon prolonged exposure to the acidic vapours, or slowly (*ca* 6 months-1 year) upon encapsulation in a vial in air. The structure of **5b** was determined from powder diffraction data; the good fit observed following Rietveld refinement ( $R_{\text{wp}} = 0.0497$ ) demonstrates the validity of the model. **5b**, like **5a**, adopts a triclinic cell with space group  $P\bar{1}$  and an almost identical asymmetric unit to that of **5a** with the copper ion on an inversion centre and similar pairs of  $\text{Cu-Cl}$  distances ( $\text{Cu-Cl } 2.2501(3)$  Å and  $2.2955(3)$  Å). The hydrogen bonding arrangement in **5a** is very similar to that in **5b**. The

H-INAm pyridinium group forms a similar  $R_1^2(4)$  motif through two N-H $\cdots$ Cl hydrogen bonds (N $\cdots$ Cl 3.1537(4) Å and 3.1825(3) Å) and the common  $R_2^2(8)$  interaction composed of two amide groups is also present (N $\cdots$ O 2.8919(3) Å), although the  $C_3^3(18)$  chains produced by these two components run in the  $[\bar{1}21]$  direction, as shown in Figure 7A. The hydrogen bonded sheets created by the chain interactions and additional N-H $\cdots$ Cl contacts between amine moieties and Cl ions (N $\cdots$ Cl 3.3155(4) Å) are parallel to the  $(11\bar{1})$  plane; the chains which make up these sheets are slightly offset from each other compared to **5a**. The main difference between the two polymorphs is how the sheets stack. In **5a**, the sheets are positioned such that Cu displays a 4+2 coordination geometry with four Cl ions and two O atoms; in contrast, the sheets in **5b** arrange themselves so that chloride ions belonging to cuprate ions of sheets above and below in the  $[310]$  direction form much longer and weaker Cu-Cl coordinate bonds (3.206(5) Å) instead, seen in Figure 7B, giving a homoleptic 4+2 geometry of six chloride ions. It is highly probable that the rearrangement of **5b** to **5a** occurs by the cleavage of the long Cu-Cl interaction, shifting of alternate sheets past each other such that the arrangement of matches that found in **5a**, then formation of long Cu-O bonds. The most likely movement in this rearrangement is the one with the shortest pathway which would be a shift of approximately 3.4 Å of alternate sheets in the  $[101]$  direction, with every other sheet moving a similar distance in the opposite direction.

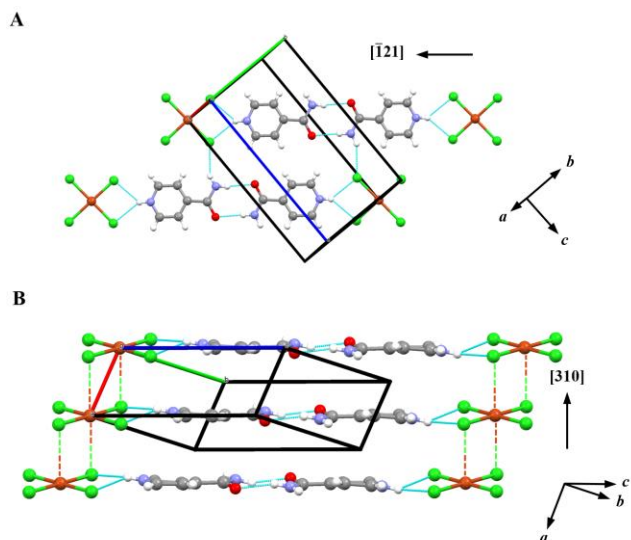


**Figure 7.** A view of the hydrogen bonded sheets in  $[\text{CuCl}_4](\text{H-INAm})_2$  (Form II) (**5b**) as viewed normal to the plane showing the  $\text{C}_3^3(18)$  chain interactions that extend in the  $[\bar{1}21]$  direction, and the additional  $\text{N-H}\cdots\text{Cl}$  contacts that link them (A). The stacking arrangement of the sheets in the  $[310]$  direction that produce a copper halide polymer that extends along  $a$  by formation of long  $\text{Cu-Cl}$  bonds drawn as dashed lines (B). Hydrogen bonds are drawn as light-blue dashed lines.

The fact that **5b** is the initial product of the solid-gas reaction and slowly transforms into **5a**, coupled with the knowledge that **5a** appears as the only product crystallised from solution leaves us with the conclusion that **5b** is the kinetic product and **5a** the thermodynamic product. **5a** and **5b** both convert to **2** when left in an open container through loss of  $\text{HCl}$  in about 3 days.

There is only one tetrachloroplatinate salt of isonicotinamide reported by Adams *et al.* The structure displays similar hydrogen bonded sheets to those in **5a** and **5b**, however the sheets are arranged differently as it is not favourable for  $\text{Pt}$  to form additional coordination bonds unlike  $\text{Cu}$ . This is similar to the observation made when comparing the anhydrous Isonicotinic acid  $\text{PtCl}_4$  and  $\text{CuCl}_4$  salts.

Another interesting observation is that grinding of **5b** with hydrochloric acid, or  $\text{CuCl}_2 \cdot 2\text{H}_2\text{O}$  with two molar equivalents of  $\text{INAm} \cdot \text{HCl}$ , or  $\text{CuCl}_2 \cdot 2\text{H}_2\text{O}$  with  $\text{INAm}$  in a 1:2 molar ratio with several drops of hydrochloric acid produces a compound which displays a different X-ray powder diffraction pattern to that of **5a** and **5b**. We were able to index the pattern and perform a satisfactory Pawley refinement ( $R_{\text{wp}} = 0.0904$ ,  $\chi^2 = 3.834$ ). This showed that the compound possesses a triclinic unit cell of dimensions  $a = 9.12(2) \text{ \AA}$ ,  $b = 12.34(3) \text{ \AA}$ ,  $c = 12.42(3) \text{ \AA}$ ,  $\alpha = 68.92(1)^\circ$ ,  $\beta = 82.21(1)^\circ$ ,  $\gamma = 72.37(1)^\circ$ ,  $V = 1243(5) \text{ \AA}^3$ . The volume is approximately triple that of **5a** and **5b**. Assuming there is a centre of symmetry this equates to one and a half  $\text{CuCl}_4$  units and three molecules of  $\text{INAm}$ . This is a very difficult structural problem to solve, and consequently we have been unsuccessful in our attempts to produce a solution. The structure requires much more computational time and potentially better quality data to solve.

**Cuprate compounds and solid-gas reactions of nicotinamide.** The cuprate  $[\text{CuCl}_4](\text{H-NAm})_2$  (Form I), **6a**, crystallises out from a concentrated hydrochloric acid solution of the same reagents which produce  $[\text{CuCl}_2(\text{NAm})_2]$ , **3**. Structure determination by single crystal diffraction shows that **6a** adopts the orthorhombic space group  $Pca2_1$ . The asymmetric unit consists of two  $[\text{CuCl}_4]^{2-}$  ions which are not sited on inversion centres (Cu1-Cl 2.226(3)  $\text{ \AA}$ , 2.2321(18)  $\text{ \AA}$ , 2.261(2)  $\text{ \AA}$  and 2.278(2)  $\text{ \AA}$ ; Cu2-Cl 2.214(3)  $\text{ \AA}$ , 2.2463(18)  $\text{ \AA}$ , 2.247(2)  $\text{ \AA}$  and 2.281(2)  $\text{ \AA}$ ) as well as four protonated molecules of  $\text{NAm}$  ( $\text{H-NAm}$ ) balancing the charge. Unlike the cuprates of  $\text{H-INAm}$  and  $\text{H-INAc}$ , the  $[\text{CuCl}_4]^{2-}$  units in **6a** exhibit the more common flattened tetrahedral geometry, and the hydrogen bonding arrangements are much more complex and unpredictable than the previous cuprate salts, though can be deconvoluted into two basic interactions occurring along the  $a$  axis. The first of these is the  $C_2^2(6)$  interactions formed by each protonated nicotinamide ion by hydrogen bonds between the amine moieties and chloride ions to create chains of cuprate ions

along *a* (N $\cdots$ Cl 3.3315(2) Å, 3.3358(2) Å, 3.3855(1) Å, 3.4127(1) Å, 3.4164(1) Å, 3.4227(1) Å, 3.4542(2) Å and 3.4852(2) Å), seen in Figure 8A. The second is a C<sub>1</sub><sup>1</sup>(6) interaction between the pyridinium and carboxyl moieties of neighbouring H-NAm molecules (N $\cdots$ O 2.6545(2) Å, 2.6731(2) Å, 2.7890(2) Å and 2.8012(2) Å), shown in Figure 8B. It is important to note that while the second interaction occurs between adjacent H-NAm molecules, it is only alternate ones which are involved in the first interaction for a particular chain of hydrogen bonded cuprates. The second interaction is also bifurcated for two of the H-NAm molecules in the asymmetric unit, those which form the longest N-H $\cdots$ O contacts, such that the pyridinium hydrogen sits between the carboxyl oxygen and the chloride of a cuprate ion (N $\cdots$ Cl 3.2556(1) Å and 3.2603(1) Å). These interactions combine to produce two similar 2-D hydrogen bonded frameworks related by a non-crystallographic centre of inversion, each composed of one [CuCl<sub>4</sub>]<sup>2-</sup> and two H-NAm ions. The two frameworks stack along *c* in an interlocking zip-like fashion shown in Figure 8C.

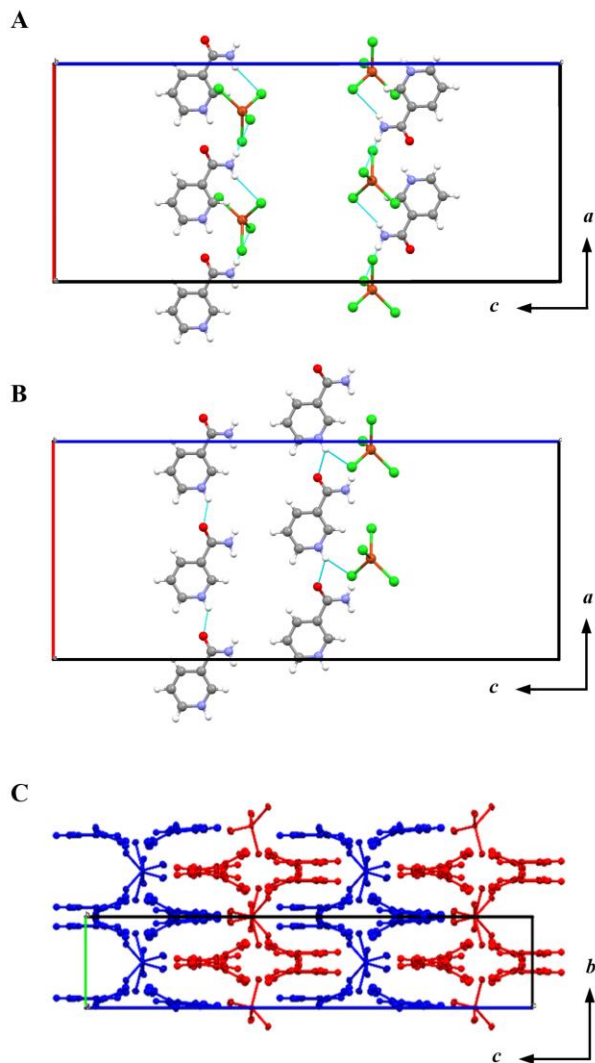
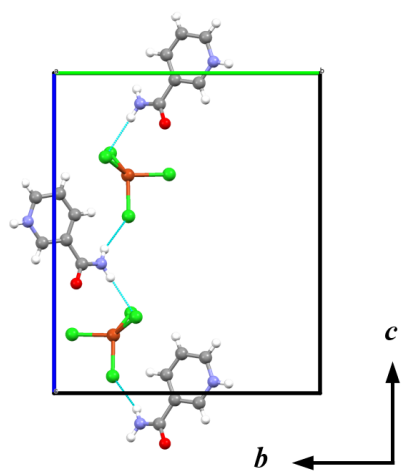
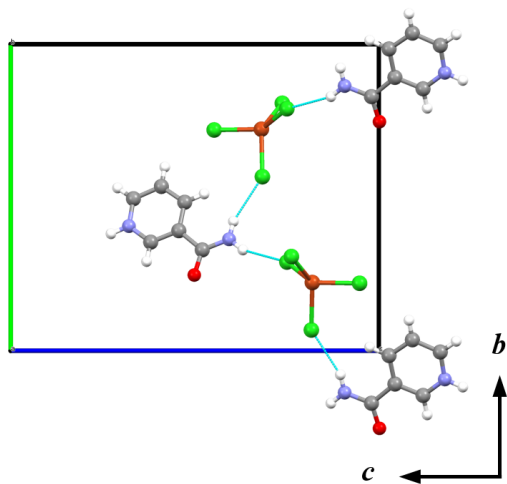


**Figure 8.** A view of the  $\text{C}_2^2(6)$  amine-cuprate (A), and  $\text{C}_1^1(6)$  nicotinamide-nicotinamide (B) hydrogen bonded chains that occur along the  $a$  axis in  $[\text{CuCl}_4](\text{H-NAm})_2$  (Form I) (**6a**). Also pictured is the shape of the two 2-D hydrogen bonded frameworks coloured in red and blue to show how they pack together in the structure (C). Hydrogen bonds are drawn as light-blue dashed lines.

The reaction of **3** with hydrochloric acid vapour produces a yellow compound with a diffraction pattern different from that of **6a**. An acidified (HCl) acetonitrile solution of  $\text{CuCl}_2$  and NAM

produced yellow crystals with the same diffraction pattern. Single crystal X-ray diffraction showed this to be  $[\text{CuCl}_4](\text{H-NAm})_2$  (form II), **6b**. This crystallises with the space group  $P2_1/c$ , and contains only one  $[\text{CuCl}_4]^{2-}$  (Cu-Cl 2.2429(5) Å, 2.2433(4) Å, 2.2545(5) Å and 2.2614(5) Å) and two H-NAm ions in the asymmetric unit. The array of hydrogen bonding motifs in **6a** and **6b** is remarkably similar; the main difference is in the orientation of the amide group which is oriented with the amine closest to the pyridine N in **6a** and the opposite in **6b** resulting in a substantially different structure. The amine-cuprate chain ( $\text{N}\cdots\text{Cl}$  3.246(2) Å, 3.262(2) Å, 3.302(1) Å and 3.341(2) Å) is present as two crystallographically distinct  $\text{C}_2^2(6)$  interactions along  $b$  and  $c$ , shown in Figure 9A. The pyridinium-carboxyl interaction is also present ( $\text{N}\cdots\text{O}$  2.679(2) Å and 2.709(2) Å) as a  $\text{C}_2^2(12)$  interaction along  $b$ , displayed in Figure 9B; this is double the length of the similar  $\text{C}_1^1(6)$  interaction found in **6a** as both of the H-NAm cations in the asymmetric unit are involved in a singular arrangement.

**A**



**B**

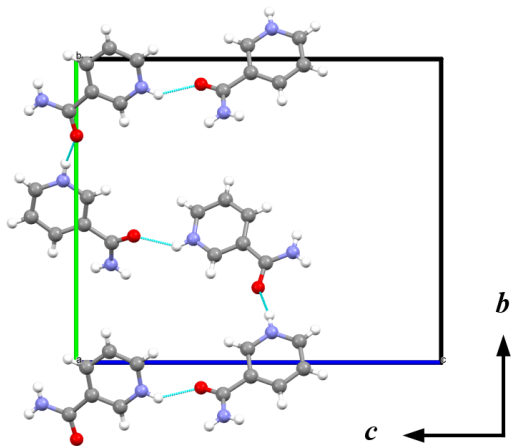


**Figure 9.** A view of the  $C_2^2(6)$  amine-cuprate chains along the  $b$  and  $c$  axes (A), and the  $C_2^2(12)$  interactions that occur along the  $b$  axis produced by the nicotinamide molecules in  $[CuCl_4](H-NAm)_2$  (form II) (**6b**) (B). Hydrogen bonds are drawn as light-blue dashed lines.

Figure 10 shows the main difference between the two polymorphs; the orientation of the amide group with respect to the pyridinium ring. In **6a** the amide is orientated with the amine closest to the pyridinium N, whereas in **6b** the carboxyl group is closer. Interestingly, the amide orientations in **3** and **6b** match, **6b** being the product of reaction of **3** with concentrated hydrochloric acid vapour. Additionally, the product of grinding nicotinamide hydrochloride with copper chloride is pure **6a**, and again the starting reagent,  $NAm.HCl$ , has the same orientation of the amide as the product. This leaves us with the conclusion that the amide orientation of the starting reagent controls which cuprate polymorph is produced, indicating that the relative stability of the two cuprates must be very similar, or at least greater than the energy required to reconfigure the  $NAm$  molecule in the solid-state. The loss of  $HCl$  from **6a** and **6b**, on the other hand, produces only **3** in about 3 days. The most probable reason for this is that **3** is the most thermodynamically favoured structure, no polymorph exists with the amide oriented as in **6b**.

The tetrachloroplatinate salt of nicotinamide displays similar hydrogen bonding motifs to those observed in **6a** and **6b**, however the overall structure is substantially different due to the square planar coordination of  $Pt$ .

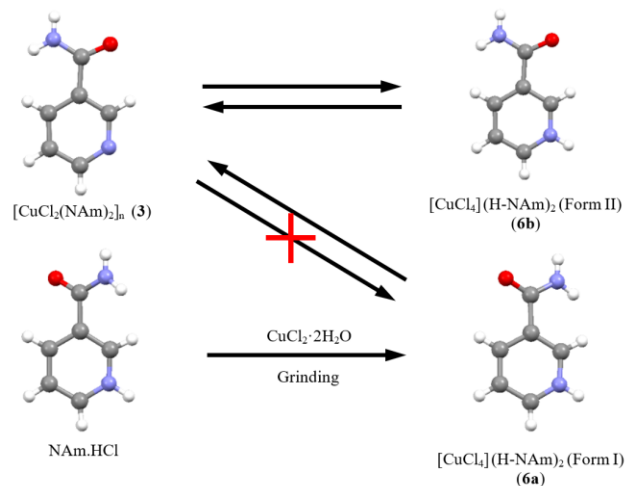


**Figure 10.** The effect of amide orientation in the starting material on controlling which cuprate polymorph of NAM is produced via solid-state reaction.

**Reaction rate.** Brammer *et al.* found that  $[\text{CuCl}_2(3\text{-Clpy})_2]$  and  $[\text{CuCl}_2(3\text{-Brpy})_2]$  react with hydrochloric acid vapour to produce the corresponding cuprate in about 2 days, the reverse reaction taking 1 day and 7 days respectively.<sup>17</sup> They also reported that a similar compound produced with 2-(imidazol-2-yl)pyridine reacts with HCl to completion in 1 hour with a similar setup, though did not report on the reverse reaction.<sup>21</sup> **1**, **2** and **3** react with the acidic vapours completely in about 3 hours each, and the reverse reaction to lose HCl gas takes about 2-3 days. A few possible explanations for these observed reaction rates are differences in particle size, ligand acidity and the strength of intermolecular interactions or crystal packing.

Particle size could have a large effect on the rate as larger particles will have a smaller surface area per volume and thus presumably react at a slower rate. To address the role of particle size in this work, SEM images of the compounds both before and after HCl inclusion were taken which are contained in the supporting information. Overall it appears as if there is a change in shape rather than size during the process of HCl absorption. **1** has crystallite of approximate size 1-6  $\mu\text{m}$  but

also some that are much smaller below 1  $\mu\text{m}$ . These smaller crystallites are not present after reaction with HCl. The crystallites in **2** are about 1-2  $\mu\text{m}$  in size before and after exposure to HCl, and the shapes are very similar. However, some rounding of the edges occurs upon reaction making them much less defined than in the initial sample. **3** also appears to show little change in size upon reaction; the average crystallite size is in the range 0.5-1  $\mu\text{m}$  before, and 0.5-2  $\mu\text{m}$  after reaction with HCl, but there is a clear change in shape. Initially the crystallites appear acicular, but upon treatment with HCl they become more block-like. The difference in particle size between **1**, **2**, and **3**, and **4b**, **5b**, and **6b** is not great, meaning the observed reaction times are more likely a result of chemical rather than physical properties of the samples. However, a more thorough study of the effect of particle size on reaction rate would be required to rule it out entirely as a contributing factor, which is beyond the scope of the present work. The absence of significant changes in crystallite size augurs against a complete dissolution-reprecipitation mechanism. However, the clear change in crystal surface morphology suggests there is some dissolution occurring. One possible mechanism is the absorption of HCl on the surface of the crystallites and a reorganization near the surface. HCl then permeates through the sample until complete conversion occurs.

Ligand acidity, *i.e.* the ability to gain and lose protons, could also play a role in determining reaction rate as a basic ligand is more likely to accept a proton than a more acidic one, and potentially displays an increased reaction rate given the same conditions. The evidence found thus far shows that the acidity or  $\text{pK}_a$  of the ligands (referring to the reaction  $\text{R-C}_3\text{H}_5\text{N-H}^+ \rightleftharpoons \text{R-C}_3\text{H}_5\text{N} + \text{H}^+$ ) is a poor indicator for reaction rate. INAc is substantially more acidic than INAm and NAM ( $\text{pK}_a = 1.77, 3.61$  and  $3.40$  in water for INAc, INAm and NAM respectively) yet the copper chloride compounds react at a roughly similar rate. 3-Clpy and 3-Brpy are as acidic as each other ( $\text{pK}_a = 2.84$  in water), yet while they react with HCl in a similar time scale they lose HCl at

markedly different rates. However, the most basic ligand studied thus far, 2-(imidazol-2-yl)pyridine ( $pK_a = 5.54, 13.4$  in water),<sup>43</sup> also displays the fastest reaction rate for gain of HCl, so the idea of acidity controlling the reaction rate may not be entirely groundless.

Lastly, the strength of the covalent and non-covalent interactions is likely to play a large role as the structures need to distort to facilitate the movement of HCl, stronger interactions will resist distortion increasing the activation barrier for reaction thereby slowing it down. The structures investigated presently have very similar supramolecular architectures and have comparable packing densities; volume occupied per atom is 16-16.6 Å<sup>3</sup> for **1**, **2** and **3**, 17.7 Å<sup>3</sup> for **4b**, **5a**, and **5b**, and 18.6-18.9 Å<sup>3</sup> for **4a**, **6a** and **6b**. This may serve to explain why they react within similar time frames, however, for conclusive proof the mechanism by which the uptake and loss of HCl occurs needs to be understood. Brammer *et al.* have attempted to extract mechanistic information on how the halopyridine compounds react by utilising the similarity between bromide and chloride structures.<sup>18</sup> They have reacted a bromide starting material with HCl gas to create a compound with a mixed halide anion, then calculated the occupancies of chloride and bromide ions on each halide site revealing where exactly the chloride ions have ended up. They found that halide sites which took part in hydrogen or halogen bonding interactions displayed a higher occupancy for chloride than bromide ions, leading them to conclude that insertion of HCl into the Cu-N bonds causes a reorientation of the resultant cuprate anion in order to maximize intermolecular interactions. Given that HBr reacts in a similar way to HCl, a more robust method would also include reaction of the chloride starting material with HBr to exclude any effect of atom size on the mechanism. Similar studies on the newly presented compounds are required before further comments can be made on the possible role of crystal packing and intermolecular forces on reaction rate. Clearly the chemistry at work is complex and the present study does not serve to

clarify this. To elucidate the exact causes of differences in reaction rate and create a model for prediction requires a systematic study of many more compounds.

## CONCLUSIONS AND OUTLOOK

We have shown that the reactions of INAc, INAm and NAm with copper chloride in a 2:1 ratio produce similar polymeric copper chloride compounds,  $[\text{CuCl}_2(\text{INAc})_2]_n$  (**1**),  $[\text{CuCl}_2(\text{INAm})_2]_n$  (**2**), and  $[\text{CuCl}_2(\text{NAm})_2]_n$  (**3**), with almost identical supramolecular frameworks. **1**, **2** and **3** can be recrystallised from HCl(aq) to produce  $[\text{CuCl}_4](\text{H-INAc})_2(\text{H}_2\text{O})$  (**4a**),  $[\text{CuCl}_4](\text{H-INAm})_2$  (form I) (**5a**) and  $[\text{CuCl}_4](\text{H-NAm})_2$  (form I) (**6a**) respectively. However, solid-gas reaction of the same compounds with moist HCl gas produces a different set of compounds; **1** produces  $[\text{CuCl}_4](\text{H-INAc})_2$  (**4b**), **2** first yields the kinetic product  $[\text{CuCl}_4](\text{H-INAm})_2$  (form II) (**5b**) before transforming into the thermodynamic product **5a**, and **3** reacts to give  $[\text{CuCl}_4](\text{H-NAm})_2$  (form II) (**6b**). Grinding NAm.HCl with copper chloride produces **6a**, maintaining the orientation of the amide with respect to the pyridine ring of the starting material leading us to the conclusion that **6a** and **6b** must have a similar thermodynamic stability. While the cuprates **4a**, **4b**, **5a** and **5b** possess remarkable structural similarities, **6a** and **6b** differ substantially from these, though from each other only by the orientation of the amide group. All the cuprate compounds lose HCl, and water in the case of **4a**, to produce the corresponding copper halide coordination polymer. The gain and loss of HCl occurs at different rates to materials discovered previously, though the factors which control the reaction rates and the exact mechanism by which they occur still elude us. Clearly the copper chloride INAc/INAm/NAm system is very complex, and despite our extensive investigations leaves some questions unanswered and structures undetermined *e.g.* the third form of the tetrachlorocuprate salt of INAm. We hope to explore the observations made further through changing the starting materials used, *e.g.* using a different halide, metal or ligand, in order to

understand these compounds better as this may allow us to engineer materials for the controlled uptake and release of HCl, possibly for the fast, selective, visual detection of hydrohalic acids. Additionally, the resistance of copper halide-pyridine compounds to very acidic environments and the ready reversibility of reaction with hydrohalic acids provides an interesting avenue of research into porous compounds. Combination of copper halides and multitopic ligands, *e.g.* trispyridyltriazine,<sup>44</sup> may result in a variety of porous compounds with unprecedented stability, and the potential for simple reconditioning by solid-gas reaction with the relevant hydrohalic acid.

## ASSOCIATED CONTENT

**Supporting Information.** Rietveld refinement plots, ORTEP images, bond angle tables, infrared spectra, and X-Ray powder diffraction data, this material is available free of charge via the Internet at <http://pubs.acs.org>.

Atomic coordinates and refinement details for all structures have been deposited with the CCDC. CCDC 1501872-1501875 contains the supplementary crystallographic data for this single crystal structures in this paper. CCDC 1501877-1501880 contain the supplementary crystallographic data for the structures determined by *ab initio* solution from X-ray powder diffraction data. The data can be obtained free of charge from The Cambridge Crystallographic Data Centre via [www.ccdc.cam.ac.uk/structures](http://www.ccdc.cam.ac.uk/structures).

## AUTHOR INFORMATION

### Corresponding Author

\*t.prior@hull.ac.uk

## Author Contributions

All authors have given approval to the final version of the manuscript.

## ACKNOWLEDGMENTS

The authors thank the University of Hull for funding of a studentship to SMF under the 80<sup>th</sup> Anniversary Studentship Scheme.

## REFERENCES

- (1) Furukawa, H.; Cordova, K. E.; O’Keeffe, M.; Yaghi, O. M. *Science* **2013**, *341*, 974.
- (2) Suh, M. P.; Park, H. J.; Prasad, T. K.; Lim, D.-W. *Chem. Rev.* **2012**, *112*, 782–835.
- (3) Li, J.-R.; Ma, Y.; McCarthy, M. C.; Sculley, J.; Yu, J.; Jeong, H.-K.; Balbuena, P. B.; Zhou, H.-C. *Coord. Chem. Rev.* **2011**, *255*, 1791–1823.
- (4) Takamizawa, S.; Nataka, E.; Akatsuka, T.; Miyake, R.; Kakizaki, Y.; Takeuchi, H.; Maruta, G.; Takeda, S. *J. Am. Chem. Soc.* **2010**, *132*, 3783–3792.
- (5) Xiao, B.; Byrne, P. J.; Wheatley, P. S.; Wragg, D. S.; Zhao, X.; Fletcher, A. J.; Thomas, K. M.; Peters, L.; Evans, J. S. O.; Warren, J. E.; Zhou, W.; Morris, R. E. *Nat. Chem.* **2009**, *1*, 289–294.
- (6) Lennartson, A.; Salo, K.; Håkansson, M. *Acta Crystallogr.* **2005**, *E61*, m1261–m1263.
- (7) Kelley, A.; Nalla, S.; Bond, M. R. *Acta Crystallogr. Sect. B Struct. Sci. Cryst. Eng. Mater.* **2015**, *71*, 48–60.
- (8) Neve, F.; Francescangeli, O.; Crispini, A.; Charmant, J. *Chem. Mater.* **2001**, *13*, 2032–2041.
- (9) Adams, C. J.; Crawford, P. C.; Orpen, A. G.; Podesta, T. J.; Salt, B. *Chem. Commun.* **2005**, *10*, 2457–2458.

- (10) Adams, C. J.; Colquhoun, H. M.; Crawford, P. C.; Lusi, M.; Orpen, A. G. *Angew. Chemie Int. Ed.* **2007**, *46*, 1124–1128.
- (11) Adams, C. J.; Gillon, A. L.; Lusi, M.; Orpen, A. G. *CrystEngComm* **2010**, *12*, 4403.
- (12) Adams, C. J.; Haddow, M. F.; Lusi, M.; Orpen, A. G. *Proc. Natl. Acad. Sci. U. S. A.* **2010**, *107*, 16033–16038.
- (13) Chen, W.-T.; Luo, Z.-G.; Xu, Y.-P.; Luo, Q.-Y.; Liu, J.-H. *J. Chem. Res.* **2011**, *35*, 253–256.
- (14) Lah, N.; Leban, I. *Acta Crystallogr.* **2005**, *E61*, m1708–m1710.
- (15) Marsh, W. E.; Valente, E. J.; Hodgson, D. J. *Inorganica Chim. Acta* **1981**, *51*, 49–53.
- (16) Adams, C. J.; Lusi, M.; Mutambi, E. M.; Orpen, A. G. *Chem. Commun.* **2015**, *51*, 9632–9635.
- (17) Espallargas, G. M.; Brammer, L.; Van De Streek, J.; Shankland, K.; Florence, A. J.; Adams, H. *J. Am. Chem. Soc.* **2006**, *128*, 9584–9585.
- (18) Mínguez Espallargas, G.; van de Streek, J.; Fernandes, P.; Florence, A. J.; Brunelli, M.; Shankland, K.; Brammer, L. *Angew. Chemie Int. Ed.* **2010**, *49*, 8892–8896.
- (19) Vitorica-Yrezabal, I. J.; Sullivan, R. A.; Purver, S. L.; Curfs, C.; Tang, C. C.; Brammer, L. *CrystEngComm* **2011**, *13*, 3189–3196.
- (20) Mínguez Espallargas, G.; Florence, A. J.; van de Streek, J.; Brammer, L. *CrystEngComm* **2011**, *13*, 4400–4404.
- (21) Coronado, E.; Giménez-Marqués, M.; Brammer, L.; Espallargas, G. M. *Nat. Commun.* **2012**, *3*, 1–8.
- (22) Sinha, A. S.; Rao Khandavilli, U. B.; O'Connor, E. L.; Deadman, B. J.; Maguire, A. R.; Lawrence, S. E. *CrystEngComm* **2015**, *17*, 4832–4841.

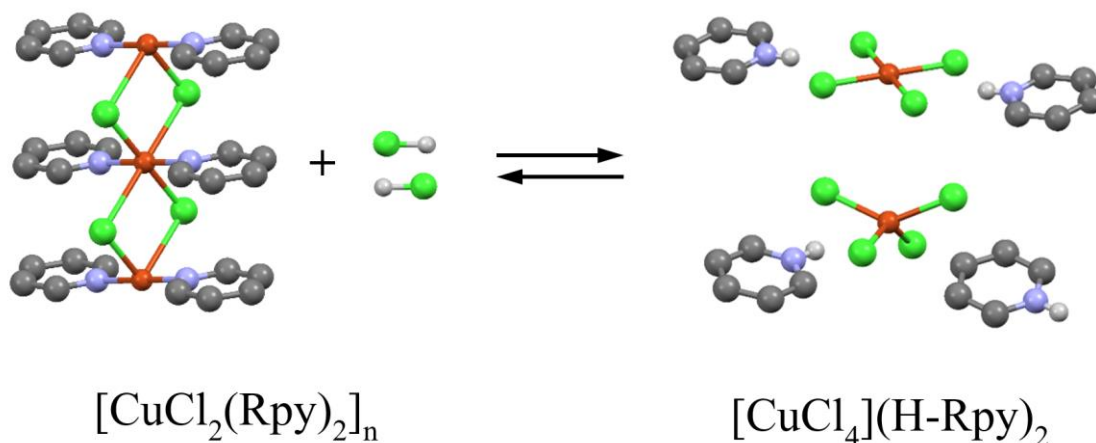
- (23) Fellows, S. M.; Prior, T. J. *Acta Crystallogr. Sect. E Crystallogr. Commun.* **2016**, *72*, 436–439.
- (24) Karki, S.; Friščić, T.; Jones, W. *CrystEngComm* **2009**, *11*, 470–481.
- (25) Adams, C. J.; Angeloni, A.; Orpen, A. G.; Podesta, T. J.; Shore, B. *Cryst. Growth Des.* **2006**, *6*, 411–422.
- (26) Gubin, A. I.; Nurakhmetov, N. N.; Buranbaev, M. Z.; Mul’kina, R. I.; Erkasov, R. S. *Kristallografiya* **1989**, *34*, 238–239.
- (27) Krishna Kumar, D.; Ballabh, A.; Amilan Jose, D.; Dastidar, P.; Das, A. *Cryst. Growth Des.* **2005**, *5*, 651–660.
- (28) CrysAlisPro 1.171.38.23t: Agilent Technologies Ltd, Yarnton, Oxfordshire, England, 2014.
- (29) X-Area, X-Red, X-Red32, X-Shape: Stoe & Cie, Darmstadt, Germany, 2012.
- (30) Farrugia, L. J. *J. Appl. Cryst.* **2012**, *45*, 849–854.
- (31) Sheldrick, G. M. *Acta Cryst.* **2015**, *A71*, 3–8.
- (32) Sheldrick, G. M. *Acta Cryst.* **2015**, *C71*, 3–8.
- (33) Spek, A. L. *Acta Cryst.* **2009**, *D65*, 148–155.
- (34) HighScore Plus (3.0e (3.0.5)): PANalytical, Almelo, The Netherlands, 2012.
- (35) Brandenburg, K.; Putz, H. Endeavour - Structure Solution from Powder Diffraction (1.7g): Crystal Impact GbR, Bonn, Germany, 2015.
- (36) Allen, F. H. *Acta Cryst.* **2002**, *B58*, 380–388.
- (37) Toby, B. H. *J. Appl. Cryst.* **2001**, *34*, 210–213.
- (38) Qin, Z.; Jenkins, H. A.; Coles, S. J.; Muir, K. W.; Puddephatt, R. J. *Can. J. Chem.* **1999**, *77*, 155–157.
- (39) Ryo Sekiya, Shin-ichi Nishikiori, Ogura, K. **2004**.

- (40) Sekiya, R.; Nishikiori, S. *Chem. - A Eur. J.* **2002**, *8*, 4803–4810.
- (41) Xue, J.; Hua, X.; Yang, L.; Li, W.; Xu, Y.; Zhao, G.; Zhang, G.; Liu, L.; Liu, K.; Chen, J.; Wu, J. *J. Mol. Struct.* **2014**, *1059*, 108–117.
- (42) Sekiya, R.; Nishikiori, S.; Kuroda, R. *CrystEngComm* **2009**, *11*, 2251.
- (43) Boggess, R. K.; Martin, R. B. *Inorg. Chem.* **1974**, *13*, 1525–1527.
- (44) Biedermann, H. G.; Wichmann, K. *Z. Naturforsch., B Anorg. Chem. Org. Chem.* **1974**, *29*, 360–362.

For Table of Contents Use Only

Polymorphism and solid-gas/solid-solid reactions of isonicotinic acid, isonicotinamide, and nicotinamide copper chloride compounds

Simon M. Fellows and Timothy J. Prior



**Synopsis**

Isonicotinic acid, isonicotinamide and nicotinamide react with copper chloride to produce coordination polymers with similar supramolecular frameworks, which react reversibly with HCl to give tetrachlorocuprate salts. The polymorphism, structural interconversion and mechanochemical synthesis of these compounds is described.